Materials and Interfaces

Eco-friendly fabrication of highly selective amide-based polymer for CO capture

Kehinde Fayemiwo, Nutchapon Chiarasumran, Seyed Ali Nabavi, Konstantin Loponov, Vasilije Manovic, Brahim Benyahia, and Goran T. Vladisavljevic

Ind. Eng. Chem. Res., **Just Accepted Manuscript** • DOI: 10.1021/acs.iecr.9b02347 • Publication Date (Web): 05 Sep 2019

Just Accepted

is published by the American Chemical Society. 1155 Sixteenth Street N.W., Washington, DC 20036

Industrial and Engineering Chemistry Research, Volume 58, Issue 39, October 2019, pp. 18160−18167
DOI:10.1021/acs.iecr.9b02347

Eco-friendly fabrication of highly selective amide-based polymer for CO_2 capture

Kehinde A. Fayemiwo[1], *Nutchapon Chiarasumran*[1], *Seyed A. Nabavi*[2], *Konstantin N. Loponov*[1], *Vasilije Manović*[2], *Brahim Benyahia*[1]*, *Goran T. Vladisavljević*[1]*

[1]Department of Chemical Engineering, Loughborough University, Loughborough, United Kingdom.

[2]Centre for Climate and Environmental Protection, Cranfield University, Bedford, MK43 0AL, UK.

Corresponding Author

*Corresponding author. Fax: +44 1509223923.

E-mail address: g.vladisavljevic@lboro.ac.uk (Goran T. Vladisavljević).

b.benyahia@lboro.ac.uk (Brahim Benyahia)

Department of Chemical Engineering, Loughborough University, Loughborough, LE11 3TU, United Kingdom.

ABSTRACT

Porous polymeric adsorbents for CO_2 capture (HCP-MAAMs) were fabricated by co-polymerisation of methacrylamide (MAAM) and ethylene glycol dimethacrylate (EGDMA) using acetonitrile and azobisisobutyronitrile as a porogen and initiator, respectively. The X-ray photoelectron and Fourier transform infrared spectra revealed a high density of amide groups in the polymer matrix of HCP-MAAMs, which enabled high selectivity to CO_2. The polymers BET surface area and total pore volume was up to 277 m^2 g^{-1} and 0.91 cm^3 g^{-1}, respectively. The highest CO_2 uptake at 273 K and 1 bar CO_2 pressure was 1.45 mmol g^{-1} and the heat of adsorption was 27-35 kJ mol^{-1}. The polymer with the lowest crosslinking density exhibited unprecedented CO_2/N_2 selectivity of 394 at 273 K. Life cycle assessment revealed a lower environmental impact of HCP-MAAMs compared to molecularly imprinted polymers. HCP-MAAMs are eco-friendly CO_2 adsorbents owing to their low regeneration energy, environmentally benign fabrication process, and high selectivity.

1. INTRODUCTION

Increased CO_2 releases from fossil fuel combustion resulted in global warming, which has caused adverse climate change.[1] As a consequence, strict regulation of CO_2 emissions has

been imposed[2] and considerable attention has been shifted towards developing cost-effective technologies for carbon capture.[3,4] Post-combustion capture (PCC) is the most practicable approach for capturing CO_2, as it can easily be implemented in existing large stationary sources with minimum modifications. CO_2 absorption by aqueous monoethanolamine (MEA) solutions is one of the most established PCC processes, but requires high energy for regeneration of CO_2-rich absorbent.[5] In addition, MEA and other alkyl amines are corrosive and toxic liquids that can decompose or evaporate, which renders them environmentally unsafe.[6]

Solid adsorbents such as silica, activated carbons and zeolites are interesting alternative materials for CO_2 capture due to their relatively low regeneration energy,[7–10] and suitability for fluidised bed reactors. Solid sorbents can successfully overcome the environmental issues encountered with MEA scrubbing technology and offer extremely high mass transfer surface areas per unit volume.[7] Zeolites are the most explored solid sorbents, which display a high CO_2 uptake capacity and low regeneration energy, but suffer from poor selectivity.[10,11] Namely, a high CO_2/N_2 selectivity is an important requirement for CO_2 adsorbents, which ensures high purity of the CO_2 stream after sorbent regeneration. Significant attention has recently been drawn to polymer-based materials due to their high CO_2 uptake capacities combined with good CO_2 selectivity, easy chemical modification, non-corrosiveness, and low regeneration energy.[12–18] They also possess good mechanical, thermal and physicochemical stability due to the covalent nature of the polymer networks.[12]

Conjugated microporous polymers (CMPs) with extended π-conjugation in an amorphous porous matrix have been synthesised for carbon capture.[19] The CMPs displayed a CO_2 storage capacity up to 79.3 mg g^{-1} (1.8 mmol g^{-1}) at 298 K and 1 bar and a BET surface area of 965 m^2 g^{-1} and maintained its original storage capacity after more than 20 regenerations. Recently a series of molecularly imprinted polymer (MIP) beads containing CO_2-selective nanocavities embellished with amide functional groups have been prepared and showed a relatively high selectivity of 40-50 for a 15/85 % CO_2/N_2 mixture. In addition, the polymers were produced using suspension polymerisation, which is a scalable technique, and the synthesised particles benefited from a semi-spherical morphology, resulting in a higher resistance to mechanical attrition.[20] On the other hand, the template removal after polymer synthesis is time-consuming and generates a substantial amount of waste due to the large volume of toxic solvent required, which makes the process expensive and less environmentally friendly.

In our previous study, hypercrosslinked polymethacrylamide-based sorbents with a CO_2:N_2 selectivity of 104 at ultra-low CO_2 pressures were synthesised.[21] In this work, we have developed eco-friendly amide-based polymers with a very high CO_2 selectivity of 394 towards a gas mixture containing 15 wt% CO_2 at 1 bar and 273 K. Life cycle assessment (LCA) was performed to compare the impacts on the environment of the synthesised polymers and the previously synthesised MIPs. The polymers were produced by bulk polymerisation method as it is the simplest method of production that does not require specialised equipment. In addition, the polymers fabricated via this method are pure, without any traces of surfactant.

2. EXPERIMENTAL SECTION

2.1. Materials

Analytical grade methacrylamide (MAAM), ethylene glycol dimethacrylate (EGDMA) and azobisisobutyronitrile (AIBN) were purchased from Sigma Aldrich (UK) and used as the monomer, crosslinker, and thermal radical initiator, respectively. Analytical grade acetonitrile (ACN) was supplied by Fisher Scientific (UK) and used as the porogen. A Milli-Q Plus 185 water purifier was used to generate pure water. CO_2 and N_2 gases with a purity above 99.999% were supplied by BOC (UK).

2.2. Particle Fabrication

Porous poly(methacrylamide-co-ethylene glycol dimethacrylate) adsorbents (HCP-MAAMs) were synthesised by dissolving 24 mmol MAAM, 20-60 mmol EGDMA, and 0.6 mmol AIBN in 20-40 mL of ACN (Table 1). ACN was selected as the porogenic solvent, since it provides a high solubility for AIBN, EGDMA, and MAAM. Moreover, ACN is highly compatible with the resulting polymer, leading to a delayed onset of phase separation and formation of small pores. Finally, ACN is less toxic when compared with dimethyl sulfoxide, dimethylformamide, and toluene. The mixture was deaerated by ultrasonic treatment for 10 min, followed by 10 min purging with nitrogen to ensure the removal of dissolved oxygen (Figure 1). The vial containing the reaction mixture was then

hermetically closed and placed in a water bath for 24 h at 333 K to polymerise. The produced bulk polymer was ground and sieved to recover particles with the sizes ranging from 90 to 212 μm. After that, the adsorbent was rinsed with water, filtered and placed in a vacuum oven at 353 K to dry overnight.

Table 1. The specific surface area, S_{BET}, the total pore volume, V_p, and the average pore size, d_p, of the prepared samples.[a]

	EGDMA	ACN	S_{BET}	V_p	d_p
	(mmol)	(mL)	($m^2 g^{-1}$)	($cm^3 g^{-1}$)	(nm)
HCP-MAAM-2	40	30	142	0.87	29.0
HCP-MAAM-2A	40	20	193	0.47	13.8
HCP-MAAM-2B	40	40	98	0.25	12.2
HCP-MAAM-2C	20	30	4	0.01	12.6
HCP-MAAM-2D	60	30	277	0.91	16.6

[a] The amounts of AIBN and MAAM in the reaction mixture were 0.6 mmol and 24 mmol, respectively, and the polymerisation reaction proceeded for 24 h at 333 K.

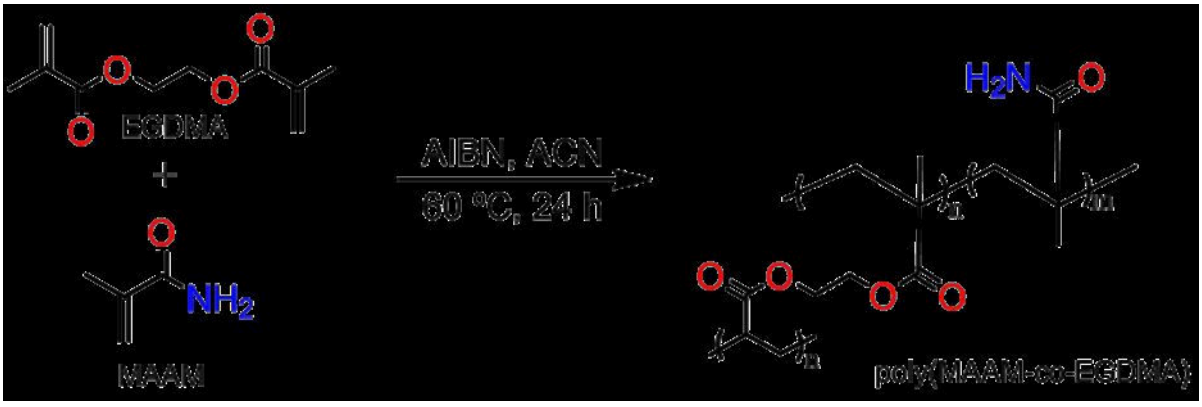

Figure 1. The schematic representation of polymerisation reaction between EGDMA and MAAM to form poly(MAAM-co-EGDMA) (HCP-MAAM).

2.3. Materials Characterisation

Pore structure analysis. The pore structure of the adsorbents was estimated using nitrogen adsorption isotherms at 77 K acquired on Micromeritics ASAP 2020 system. First, the samples were degassed at 353 K overnight and the adsorption experiments were then carried out over relative pressures ranging from 0.06 to 0.30 using the Brunauer-Emmett-Teller (BET) model. The pore size distribution was estimated using the Barrett-Joyner-Halenda (BJH) method. The total pore volume was calculated from the amount of nitrogen adsorbed at the relative pressure of 0.99.

X-Ray Photoelectron Spectroscopy (XPS). The Thermo Scientific™ K-Alpha™ system with the AVANTAGE software was used for XPS measurements. A monochromatic X-ray source (Al K_α, $h\nu$ = 1486.4 eV) was used for radiation and charge compensation. The XPS data were generated by a 400 μm diameter X-ray beam. A hemispherical analyser was used to collect the XPS spectra at 50 eV for high-resolution spectra and 200 eV for survey spectra at 0.1 eV and 1 eV steps, respectively. The background was subtracted using the Shirley methods. The peaks were fitted using the mixed Gaussian-Lorentzian peak shape with 30% Lorentzian character.[22]

Fourier Transform Infrared (FT-IR) Spectroscopy. FT-IR spectra were obtained using a Nicolet iS50ATR-FTIR spectrometer (Thermo Scientific) with a monolithic diamond crystal, equipped with OMNIC 7 software. For each measurement, about 2-3 mg of the polymer was placed onto the universal diamond ATR top-plate. The measurements were repeated five times and the spectra based on mean values were used.

Thermogravimetric Analysis (TGA). The thermal stability of the adsorbents was probed using a TA Instruments Q5000IR Thermogravimetric Analyser. For each measurement, 10-20 mg of the polymer sample was exposed to a dry N_2 stream at 20 mL min^{-1} and heated from 323 K to 873 K at a rate of 10 K/min.

Density measurement. A Micromeritics helium pycnometer was used to measure the true density of the particles. Before each measurement, the samples were dried overnight under vacuum at 353 K. Each measurement was repeated three times and the mean value was calculated.

Gas adsorption. The adsorption isotherms of CO_2 and N_2 at 273 K and 298 K were estimated at gas pressures up to 100 kPa using the Micromeritics ASAP 2020. A Micromeritics ISO Controller was installed in the system to maintain a constant temperature between 273 K and 353 K during adsorption analyses. Thermoelectric cooling based on the Peltier principle was utilised to maintain a temperature of 273 K in the sample tube. Before each measurement, the adsorbent was degassed at 353 K under vacuum.

2.4. Life Cycle Assessment (LCA)

LCA is a powerful method for estimating the environmental burden of any substance during its whole life cycle.[23,24] In this study, the IMPACT 2002+ methodology was used, and the environmental impact indicators were grouped into 4 endpoint categories (Climate Change, Ecosystem Quality, Human Health, and Resources), which in turn were subdivided into 15 midpoint categories. Human Health was divided into Respiratory Inorganics, Respiratory Organics, Ionising Radiation, Carcinogens, Non-Carcinogens, and

Ozone Layer Depletion. Ecosystem Quality was divided into Terrestrial Ecotoxicity, Terrestrial Acid, Aquatic Ecotoxicity, Aquatic Acidification, Land Occupation, and Aquatic Eutrophication. Climate Change was a separate midpoint impact category and Resources category was divided into Mineral Extraction and Non-Renewable Energy. The aim of LCA was to compare the environmental impacts of seven amide-based polymeric CO_2 sorbents: five HCP-MAAMs synthesised in this work and two MIPs reported elsewhere.[19] Possible changes in the HCP-MAAMs fabrication process that can reduce their environmental footprint were also suggested. Each impact category was normalised according to the procedure described elsewhere.[25]

3. RESULTS AND DISCUSSION

3.1 Materials Characterisation

Figure 2 shows the N_2 isotherms and pore size distributions (PSDs) of HCP-MAAMs at 77 K. All samples except HCP-MAAM-2C exhibited the pseudo-type II isotherms[26] with adsorption hysteresis, but no plateau in the region of high P/P_0. Such hysteresis loops are typical for complex microporous-mesoporous materials with a broad PSD containing both micropores and mesopores.[27] A reversible monolayer adsorption in micropores was completed at $P/P_0 < 0.25$, after which multilayer N_2 adsorption and capillary condensation in mesopores were observed. The pore sizes were mainly in the range of 2-40 nm with a peak at ~4 nm. As the molar ratio of EGDMA to MAAM increased from 0.83 to 1.67 to 2.5

for HCP-MAAM-2C, HCP-MAAM-2 and HCP-MAAM-2D polymers, S_{BET} was found to increase from 4 $m^2 g^{-1}$ to 142 $m^2 g^{-1}$ to 277 $m^2 g^{-1}$, which can be explained by higher degrees of polymer crosslinking.[20,21,28] Increasing the volume of ACN used, whilst keeping all other factors constant, led to a decrease in S_{BET}, i.e. S_{BET} for HCP-MAAM-2A > S_{BET} for HCP-MAAM-2 > S_{BET} for HCP-MAAM-2B (193 $m^2 g^{-1}$ > 142 $m^2 g^{-1}$ > 98 $m^2 g^{-1}$). The formation of a porous polymer structure is a complex process involving chain propagation, crosslinking, phase separation, formation of microgel particles and aggregation of microgel particles into interconnected porous network. For the porogen contents below certain threshold level, phase separation of the polymer does not occur, and the formed polymer matrix is essentially non-porous.[29] Polymer matrix with the highest S_{BET} is formed at the threshold porogen level. As the porogen content increases further, phase separation occurs increasingly more quickly and at lower monomer conversions, which leaves more time for the microgel particles to grow and fuse together, resulting in smaller S_{BET}.

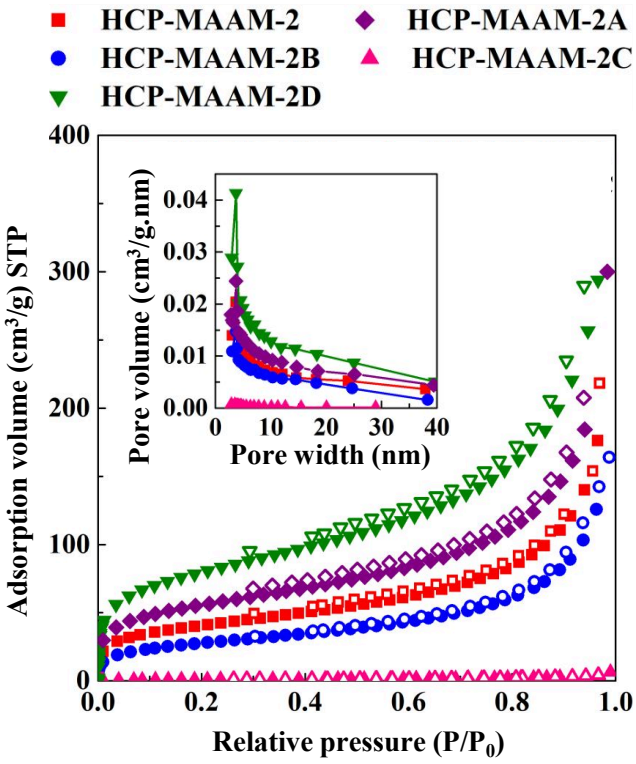

Figure 2. N_2 adsorption isotherms and pore size distributions of the samples at 77 K. All samples except HCP-MAAM-2C exhibited the pseudo-type II isotherm. The nitrogen adsorption isotherm of HCP-MAAM-2C was plotted using different y-axis scale in Figure S1 of Supplementary Information (SI).

The FT-IR spectra of the samples are shown in Figure 3a. All the spectra are characterised by a broad band at 3,400–3,500 cm^{-1} due to stretching vibrations of N-H bond and a strong sharp peak at around 1730 cm^{-1}, which can be associated to bending vibrations of N-H bond. The strong sharp peak may also be attributed to stretching vibrations of C=O bond overlapping with the N-H stretching vibrations. The strong sharp peak at 1153 cm^{-1} can be related to the C-N stretching vibrations. Thus, the $-NH_2$ groups of methacrylamide were preserved after polymerisation. Moreover, the peak corresponding to C=C band was undetected, which provides evidence that the C=C bonds of MAAM and EGDMA were broken down completely or unreacted monomer and crosslinker were completely

removed. Typical XPS survey spectra of the HCP-MAAMs and the quantification of the surface elements are shown in Figure 3b. The survey spectra of the particles showed C1s, O1s and N1s peaks. In the N1s XPS high-resolution spectra, the electron binding energy of N1s electrons revealed the -NH_2 presence in HCP-MAAMs. The presence of N1s peaks at ~400 eV confirmed that the synthesised polymers contained nitrogen. The highest percentage of nitrogen in HCP-MAAM-2C (15.2%) can be attributed to the highest MAAM-to-EGDMA ratio in this sample.[30]

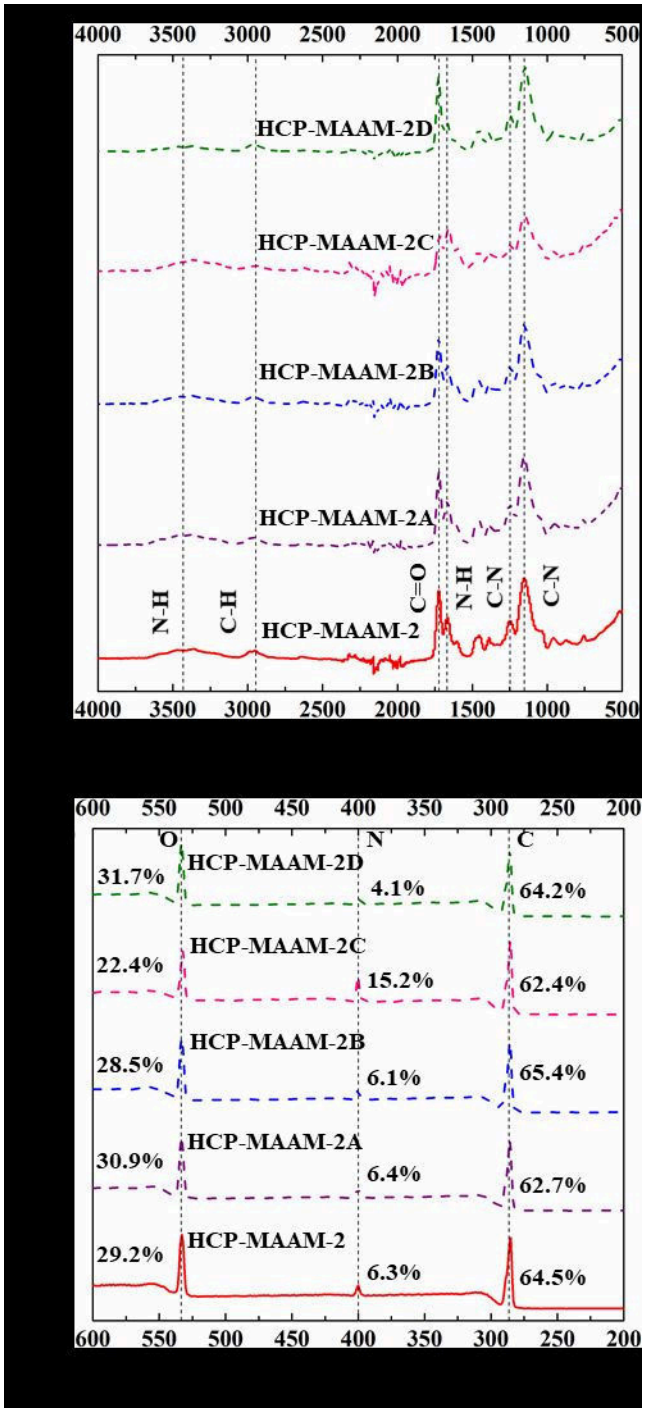

Figure 3. (a) FT-IR spectra of HCP-MAAMs; (b) XPS spectra of HCP-MAAMs and the corresponding mass percent of oxygen, nitrogen and carbon in the polymers.

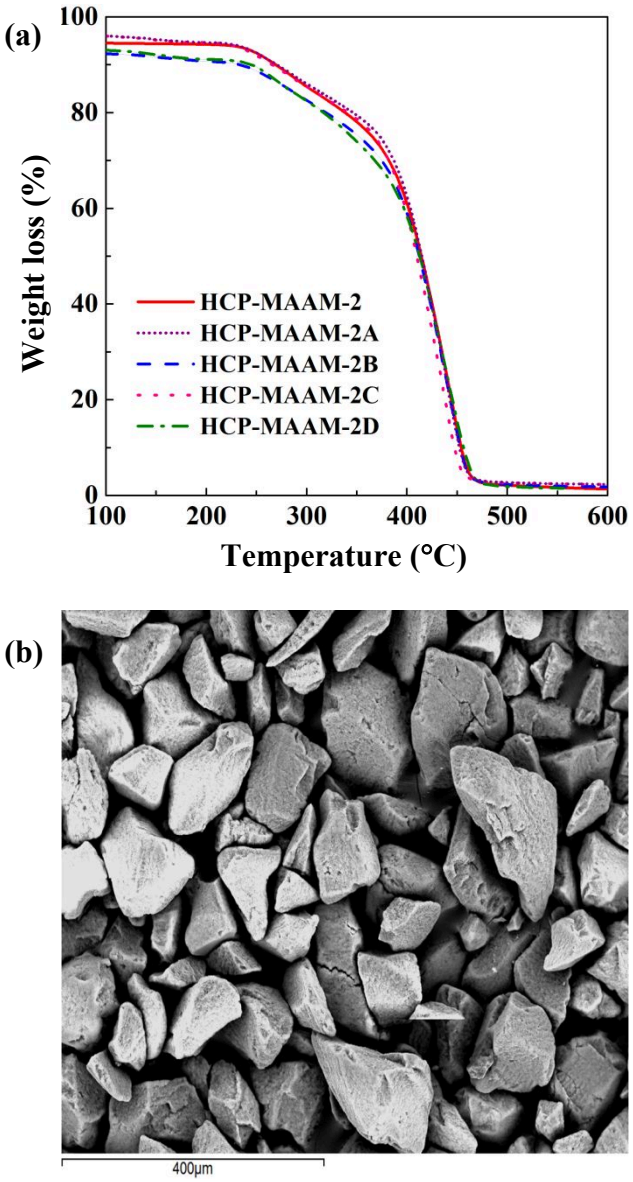

Figure 4. (a). TGA curves corresponding to sample decomposition due to heating from 100 to 600 °C; (b) SEM image of the polymer particles after grinding and sieving.

Figure 4a presents the TGA plots of the HCP-MAAMs. The onset temperature of the thermal degradation of the samples was ~250 ºC, with no significant mass loss noticed below 390 ºC. This implies high thermal stability of HCP-MAAMs and their compatibility with typical temperatures used during temperature swing adsorption (TSA). The actual density of the particles was ~1.28 g cm^{-3}. The SEM image of the particle is provided in

Figure 4b. The particles have irregular shapes formed by crushing the bulk polymer, in contrast to spherical particles formed by polymerisation of droplets.[31]

3.2 Gas Adsorption

The CO_2 and N_2 adsorption/desorption isotherms for all polymers at 273 K and 298 K are presented in Figure 5a and 5b, respectively. The CO_2 storage capacities of HCP-MAAM-2 are shown in Table 2. The CO_2 uptake capacity of HCP-MAAM-2 was slightly higher than those of covalent organic framework (COF) samples COF-8 and COF-5 of 1.43 and 1.34 mmol g^{-1} (for pure CO_2 at 1 bar and 273 K), but lower than that of COF-102 (1.56 mmol g^{-1}),[32] and those of N-enriched polymers NUT-8 (1.59 mmol g^{-1})[33] and NUT-13 (3.70 mmol g^{-1}).[34] For all samples, a decrease in temperature led to increase in CO_2 storage capacity and *vice versa*. This is expected behaviour since the materials reported here adsorb CO_2 by physisorption. The lower capture capacity was observed at the higher temperature due to the weaker polar interactions between CO_2 molecules and N-H and C=O bonds within the polymer network.

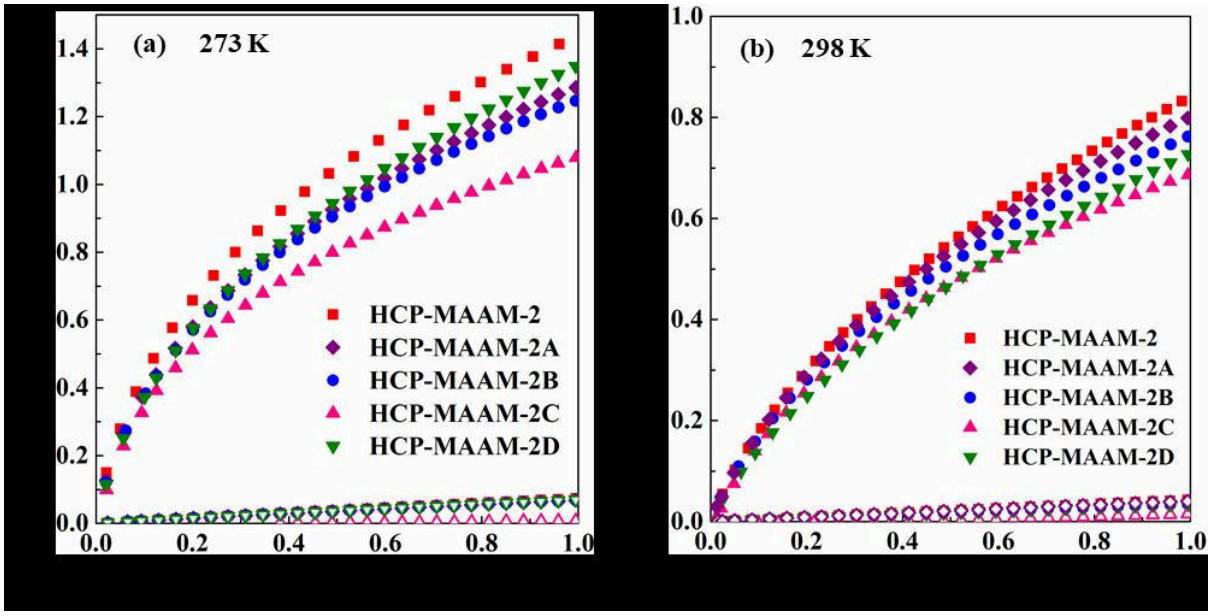

Figure 5. Adsorption isotherms of the samples at: (a) 273 K and (b) 298 K. The CO_2 and N_2 adsorption data were represented by the filled and empty symbols respectively.

The adsorption heat Q_{st} of the polymers was estimated using the Clausius-Clapeyron equation.[35] For CO_2 capture materials, Q_{st} of 30 to 50 kJ mol^{-1} are recommended, as energy penalties for sorbent regeneration are not economically viable at Q_{st} > 50 kJ mol^{-1}.[5] Figure 6 shows Q_{st} of HCP-MAAMs as a function of the amount of CO_2 adsorbed. At the start of the adsorption, the adsorbent with the highest Q_{st}, HCP-MAAM-2 had an isosteric heat of 35 kJ mol^{-1} and Q_{st} then decreased linearly to 31 kJ mol^{-1} with an increased CO_2 loading. Thus, as the CO_2 loading increased, Q_{st} significantly decreased, revealing that the degree of heterogeneity of adsorbent surface was high.[36] As pressure increased, decreasing amount of heat was released when additional adsorption sites were occupied.

For all adsorbents synthesised, Q_{st} was in the range of 27 to 35 kJ mol^{-1} when 0.15 to 0.8 mmol of CO_2 g^{-1} was adsorbed. The enthalpy of CO_2 absorption by 30 wt% MEA solution is 80 to 100 kJ mol^{-1} at 40 °C for absorption of 0.04 to 0.4 mole of CO_2 per mole of amine [37],

which is up to 3 times higher than in this study. Moreover, the enthalpies of adsorption of HCP-MAAMs reported here are 1.8–2.5 times lower than those of other CO_2 sorbents recently synthesised, such as NUT-10 [33] and bcHT-PEI-40%.[38] The smallest Q_{st} was observed for HCP-MAAM-2C in the CO_2 uptake range of 0.15 to 0.55 mmol g^{-1}, followed by HCP-MAAM-2A in the range of 0.55 to 0.8 mmol g^{-1}. The lowest Q_{st} displayed by HCP-MAAM-2C was likely due to its lowest CO_2 affinity, due to low porosity of the polymer matrix.

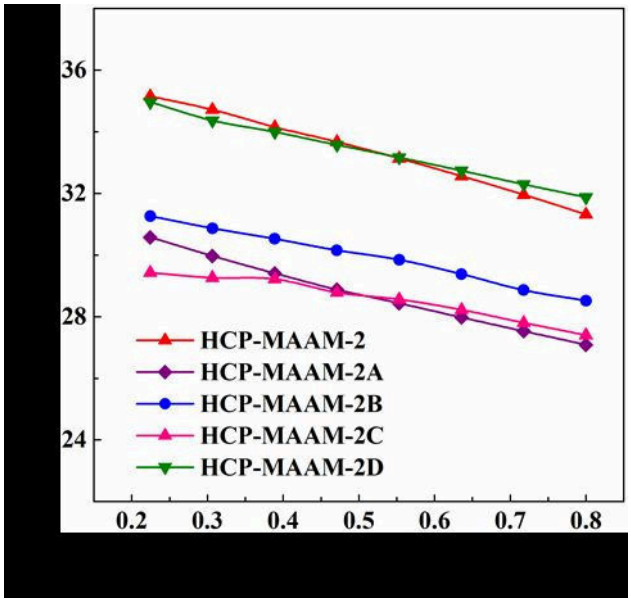

Figure 6. The heat of adsorption of the samples as a function of equilibrium CO_2 uptake.

3.3 CO_2/N_2 selectivity

Another important requirement of a good CO_2 adsorbent is the high preferential uptake of CO_2 over N_2. The selectivity was calculated at 1 bar using the ideal adsorption solution theory (IAST) as follows:

$$S = \frac{q_{CO2}/P_{CO2}}{q_{N2}/P_{N2}} \quad (1)$$

where q_i is the number of moles of gas i adsorbed per gram of polymer and p_i is the partial pressure of gas i (bar) in the feed CO_2/N_2 stream. The CO_2 stream purity after sorbent regeneration is:

$$\text{Purity} = \frac{q_{CO2}}{q_{CO2} + q_{N2}} \times 100 \quad (2)$$

The selectivities of the adsorbents at 1 bar total pressure and 273 or 298 K for a CO_2:N_2 molar ratio of 15:85 are shown in Figure S2 (SI). High CO_2/N_2 selectivity is associated with an increase in nitrogen content as previously reported.[20,21] Similar results where precursors containing amino group improved the interaction between CO_2 molecules and the pore wall contributed to the improved selectivity have been reported elsewhere.[8,33-34,38-40] The selectivity of HCP-MAAM-2 was found to be 53 at 273 K and dropped to 38 at 298 K. The corresponding purity of CO_2 stream at the two temperatures was 91% and 88% respectively. As the temperature decreases, adsorption capacity increases, while selectivity increases, which is a common adsorption behaviour.[41] HCP-MAAM-2C exhibited the highest selectivity of 394 (purity of CO_2-rich stream of 99%) and 106.9 (stream purity of 95%) at 273 and 298 K, respectively (Figure 7) at 0.15 bar CO_2 partial pressure. These selectivity values (S) are much higher than those found for PECONF-1 (S = 109 and 51 at 273 and 298 K),[42] CBZ (S = 100 and 76 at 273 and 298 K), and DBT (S = 86 and 80 at 273 and 298 K),[43] and comparable to the selectivity of Zeolite NAKA (S = 149 at 298 K).[44] The much higher selectivity of HCP-MAAM-2C as compared with other HCP-MAAMs

synthesised could have been due to its relatively small porosity, hence the gas diffusion is likely to be associated with slower kinetics, thus leading to a smaller N_2 uptake. In addition, this could be attributed to HCP-MAAM-2C high nitrogen content (15.2 %) as revealed in the XPS spectra. Thus, HCP-MAAM-2C showed moderate uptake capacities for CO_2 with a very high selectivity, high purity of CO_2 stream (95–99%), and a low heat of adsorption. This polymer can provide the required CO_2 stream purity at both 273 and 298 K without any additional purification.[45]

Table 2. CO_2 uptake capacity, selectivity, and purity of CO_2 stream released after sorbent regeneration for gas adsorption at 1 bar total pressure.

Sample	CO_2 uptake (mmol g^{-1})				CO_2:N_2 Selectivity		CO_2 stream purity (%)	
	273 K		298 K		273 K	298 K	273 K	298 K
	Pure CO_2	0.15/0.85 CO_2/N_2	Pure CO_2	0.15/0.85 CO_2/N_2	0.15/0.85 CO_2/N_2		0.15/0.85 CO_2/N_2	
HCP-MAAM-2	1.45	0.56	0.85	0.25	53	38	91	88
HCP-MAAM-2A	1.31	0.49	0.81	0.24	48	40	90	88
HCP-MAAM-2B	1.27	0.48	0.78	0.23	47	44	92	91
HCP-MAAM-2C	1.09	0.44	0.69	0.21	394	107	99	95
HCP-MAAM-2D	1.36	0.48	0.73	0.20	45	38	91	89

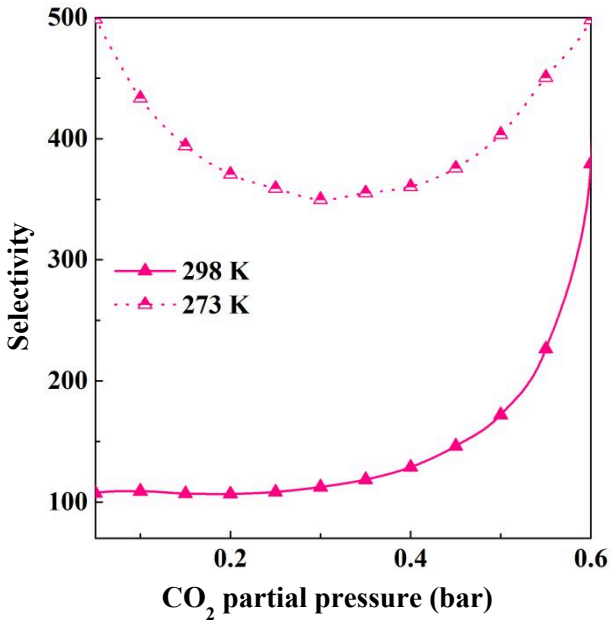

Figure 7. Selectivity of HCP-MAAM-2C at 273 K and 298 K based on IAST at CO_2:N_2 molar ratio of 15:85 and 1 bar.

3.4 Life cycle assessment (LCA) of the materials

Figure S3 (SI) summarises the amount of all chemicals (inventories) used to synthesise enough polymers to adsorb 1000 g of CO_2 overall (hereby referred to as the functional unit) in 50 cycles. It is worth noting that the amounts of sorbents considered here are different due the difference in their CO_2 uptake capacity. First, due to their enhanced CO_2 uptake capacity, the particles produced in this work require less material to capture 1 kg of carbon dioxide compared to the selected MIP particles produced by suspension polymerisation from O/O emulsions, S2-MIPs and S3-MIPs.[19] HCP-MAAM-2 requires the lowest amount of sorbent particles (0.34 kg), followed by HCP-MAAM-2D (0.37 kg), HCP-MAAM-2A (0.39 kg), HCP-MAAM-2B (0.39 kg), and HCP-MAAM-2C (0.42 kg), whereas S2-MIPs and S3-MIPs materials require 0.46 kg and 0.5 kg of the particles, respectively.

The environmental impacts of all 7 sorbents based on 1 kg of CO_2 captured at 1 bar and 273 K are presented in Figure 8a and 8b. The data were generated via SimaPro software 8.2.0 with Ecoinvent 3.0 as database. In Figures 8 and 9, the Y-axis represents a normalised impact, calculated by dividing the impact per unit of emission by the total impact of all substances within the specific category per person per year.[25] Figure 8a shows that MIPs produce much higher environmental impact across end-point categories than HCP-MAAMs. The main impact of MIPs is on depletion of natural resources and human health, mainly due to extensive use of mineral oil, which is derived from crude petroleum oil. The main impact of HCP-MAAMs is on depletion of natural resources (Figure 8b), since ACN and monomers used in the fabrication of HCP-MAAMs are synthesised from hydrocarbons derived from fossil fuels. ACN and the products of degradation of HCP-MAAMs cause very limited impacts on global warming and the human respiratory system and negligible impact on ecosystem quality. Amongst all HCP-MAAMs synthesised, HCP-MAAM-2C causes the most significant environmental impacts per 1 kg of CO_2 captured, due to the smallest CO_2 capture capacity of this polymer.

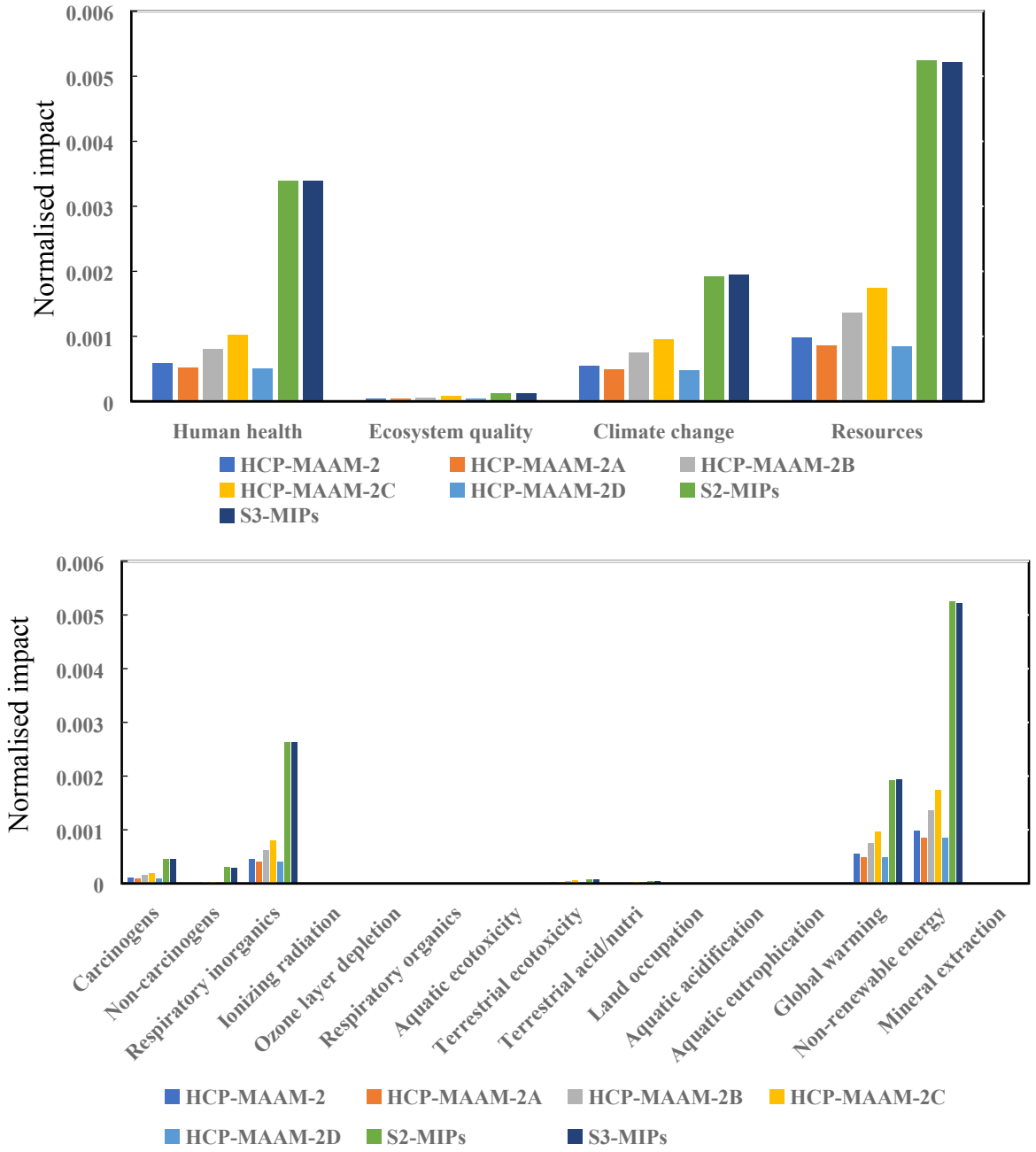

Figure 8. (a) Normalised environmental impacts (end-point categories) of the CO_2 sorbents investigated; (b) Normalised environmental impacts (mid-point categories) of all 7 sorbents.

A further investigation of the impacts of specific substances used for the synthesis of HCP-MAAM-2C and S2-MIPs were conducted. The results are shown in Figures 9a and 9b for HCP-MAAM-2C and in Figures S4 and S5 (SI) in the case of S2-MIPs.[19] The

environmental footprint of S2-MIPs is dominated by the impact of mineral oil used as a dispersion medium for reaction mixture droplets in oil-in-oil suspension polymerisation method, followed by methanol, used as a template extractant, and toluene and ACN, used as porogens. Mineral oil derives directly from crude petroleum oil and thus, its consumption causes depletion of non-renewable energy resources (Figure S5, SI). In addition, inhaling mineral oil could cause inflammation of the lungs. Other solvents also cause various respiratory, carcinogenic, and non-carcinogenic problems, as shown in Figure S5 (SI).

The environmental footprint of HCP-MAAM-2C is dominated by the impact of ACN and methacrylic acid (MCA), which is used in methacrylamide and ethylene glycol dimethacrylate synthesis and released during degradation of these chemicals. From Figure 8a, it is clear that ACN is the main environmental burden due to much higher consumption in the polymer synthesis compared to MCA (Figure S3, SI). Both ACN and MCA are produced from petrochemicals and cause depletion of non-renewable energy resources (Figure 8b). ACN can be metabolised to hydrogen cyanide and formaldehyde, which are the source of the toxic effects of ACN. Formaldehyde is a human carcinogen.

To lower the impact of ACN on the environment, it is necessary to replace ACN with greener solvents during fabrication of HCP-MAAMs[46] or to reduce the consumption of fresh solvent by recycling ACN from the wash liquid. Based on our experimental investigation, 90% of ACN can be recycled from the wastewater. In this scenario, the environmental impact of ACN would be dramatically reduced, as shown in Figures S6 and

S7 (SI). The impact on climate change can be reduced from 4.7-9.4 kg CO_2 eq. to just 1.2-2.3 kg CO_2 eq.

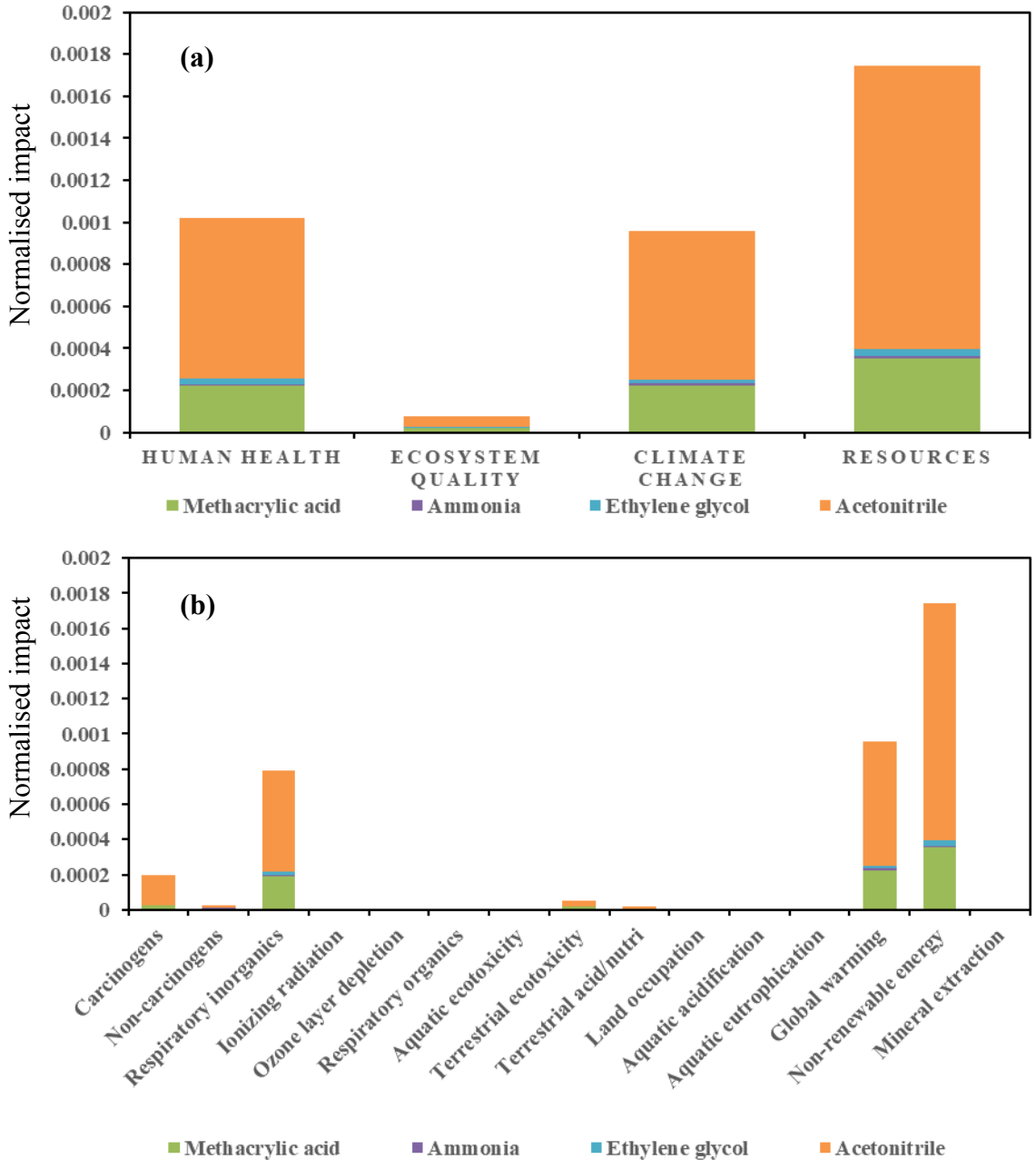

Figure 9. (a) Normalized environmental impacts (end-point categories) of HCP-MAAM-2C; (b) Normalized environmental impacts (mid-point categories) of HCP-MAAM-2C.

CONCLUSIONS

Environmentally benign polymeric sorbents for CO_2 capture made of poly[methacrylamide-co-ethylene glycol dimethacrylate] were synthesised and their adsorption properties and CO_2/N_2 selectivities were analysed. All the polymers except HCP-MAAM-2C were found to be mesoporous and displayed a pseudo-type II isotherm with a non-uniform pore size distribution and a small hysteresis loop, but no plateau in the region of high relative pressures. The S_{BET} of the polymers ranged between 98 and 277 m^2 g^{-1} and the onset temperature of thermal degradation was ~250 ºC. The polymers retained polar amide groups of methacrylamide intact and thus, there was no need for any secondary chemical modification to make them selective to CO_2.

The maximum CO_2 storage capacity of 1.45 mmol g^{-1} at 1 bar and 273 K was exhibited by HCP-MAAM-2. All the adsorbents displayed an excellent selectivity above 55 which allowed for a CO_2-reach stream purity of more than 90% after polymer regeneration at 273 K. Such high selectivity is a result of inherent nitrogen functionalisation of the monomer used in the synthesis of the adsorbents. Amongst all the adsorbents, HCP-MAAM-2C showed the highest CO_2 selectivity and the lowest heat of adsorption, with a purity of CO_2 stream after desorption step above 95%; thus, there is no need for additional gas purification before CO_2 storage. Although HCP-MAAM-2C showed a very high selectivity, for this sample to be a viable candidate to be utilised in CO_2 post combustion capture systems, the CO_2 adsorption capacity need to be further enhanced. Life cycle assessment revealed that HCP-MAAMs generate lower environmental impacts compared to molecularly imprinted

polymer sorbents (MIPs) fabricated by suspension polymerisation from oil-in-oil emulsions. No further modification of the materials is required, which minimises consumption of toxic solvents and oils. Although HCP-MAAMs have shown promising characteristics for CO_2 capture with low environmental burden, further experimentation is needed to improve their CO_2 capture capacities.

Supplementary information

- Liquid nitrogen adsorption isotherms of HCP-MAAM-2C at 77 K, CO_2/N_2 selectivity values of HCP-MAAMs at 273 K and 298 K, mass flow charts for the synthesis of 7 polymeric CO_2 sorbents per 1 kg of CO_2 captured, normalised environmental impacts of previously produced molecularly imprinted polymer particles across mid-point and end-point categories, normalized environmental impacts of HCP-MAAMs across end-point and mid-point categories in the case of 90% recycle of acetonitrile during the fabrication process.

Acknowledgements

The authors gratefully acknowledge the financial support for this work by CoERCe granted by Innovate UK, project Grant: 102213, and Cambridge Engineering and Analysis Design (CEAD) Ltd. The authors would like to thank Kim and Monika of the department of Chemical Engineering, Loughborough University for their help and support during the

entire experimental work. We would also like to thank the Loughborough Materials Characterization Centre (LMCC) for assisting in the materials characterization.

References

(1) Lee, S. Y.; Park, S. J. A Review on Solid Adsorbents for Carbon Dioxide Capture. *J. Ind. Eng. Chem.* **2015**, *23*, 1.

(2) Tseng, R. L.; Wu, F. C.; Juang, R. S. Adsorption of CO_2 at Atmospheric Pressure on Activated Carbons Prepared from Melamine-Modified Phenol–formaldehyde Resins. *Sep. Purif. Technol.* **2015**, *140*, 53.

(3) Aminu, M. D.; Nabavi, S. A.; Rochelle, C. A.; Manovic, V. A Review of Developments in Carbon Dioxide Storage. *Appl. Energy* **2017**, *208*, 1389.

(4) Bui, M.; Adjiman, C. S.; Bardow, A.; Anthony, E. J.; Boston, A.; Brown, S.; Fennell, P. S.; Fuss, S.; Galindo, A.; Hackett, L. A.; et al. Carbon Capture and Storage (CCS): The Way Forward. *Energy Environ. Sci.* **2018**, *11*, 1062.

(5) Hug, S.; Stegbauer, L.; Oh, H.; Hirscher, M.; Lotsch, B. V. Nitrogen-Rich Covalent Triazine Frameworks as High-Performance Platforms for Selective Carbon Capture and Storage. *Chem. Mater.* **2015**, *27*, 8001.

(6) Rochelle, G. T. Amine Scrubbing for CO_2 Capture. *Science* **2009**, *325*, 1652.

(7) Chang, F. Y.; Chao, K. J.; Cheng, H. H.; Tan, C. S. Adsorption of CO_2 onto Amine-Grafted Mesoporous Silicas. *Sep. Purif. Technol.* **2009**, *70*, 87.

(8) Peng, A. Z., Qi, S. C.; Liu, X.; Xue, D. M.; Peng, S. S.; Yu, G. X.; Liu, X. Q.; Sun, L. B. Fabrication of N-doped Porous Carbons for Enhanced CO_2 Capture: Rational Design of an Ammoniated Polymer Precursor. *Chem. Eng. J.* **2019**, *369*, 170.

(9) Zhao, Y.; Shen, Y.; Ma, G.; Hao, R. Adsorption Separation of Carbon Dioxide from Flue Gas by a Molecularly Imprinted Adsorbent. *Environ. Sci. Technol.* **2014**, *48*, 1601.

(10) Xiao, P.; Zhang, J.; Webley, P.; Li, G.; Singh, R.; Todd, R. Capture of CO_2 from Flue Gas Streams with Zeolite 13X by Vacuum-Pressure Swing Adsorption. *Adsorption* **2008**, *14*, 575.

(11) Loganathan, S.; Tikmani, M.; Ghoshal, A. K. Novel Pore-Expanded MCM-41 for CO_2 Capture: Synthesis and Characterization. *Langmuir* **2013**, *29*, 3491.

(12) Wang, Q.; Luo, J.; Zhong, Z.; Borgna, A. CO_2 Capture by Solid Adsorbents and Their Applications: Current Status and New Trends. *Energy Environ. Sci.* **2011**, *4*, 42.

(13) Patel, H. A.; Karadas, F.; Canlier, A.; Park, J.; Deniz, E.; Jung, Y.; Atilhan, M.; Yavuz, C. T. High Capacity Carbon Dioxide Adsorption by Inexpensive Covalent Organic

Polymers. *J. Mater. Chem.* **2012**, *22*, 8431.

(14) Xiang, Z.; Mercado, R.; Huck, J. M.; Wang, H.; Guo, Z.; Wang, W.; Cao, D.; Haranczyk, M.; Smit, B. Systematic Tuning and Multi-Functionalization of Covalent Organic Polymers for Enhanced Carbon Capture. *J. Am. Chem. Soc.* **2015**, *137*, 13301.

(15) Chen, X.; Qiao, S.; Du, Z.; Zhou, Y.; Yang, R. Synthesis and Characterization of Functional Thienyl-Phosphine Microporous Polymers for Carbon Dioxide Capture. *Macromol. Rapid Commun.* **2013**, *34*, 1181.

(16) Gu, C.; Huang, N.; Chen, Y.; Qin, L.; Xu, H.; Zhang, S.; Li, F.; Ma, Y.; Jiang, D. π-Conjugated Microporous Polymer Films: Designed Synthesis, Conducting Properties, and Photoenergy Conversions. *Angew. Chemie Int. Ed.* **2015**, *54*, 13594.

(17) Nabavi, S. A.; Vladisavljević, G. T.; Wicaksono, A.; Georgiadou, S.; Manović, V. Production of Molecularly Imprinted Polymer Particles with Amide-Decorated Cavities for CO_2 Capture Using Membrane Emulsification/Suspension Polymerisation. *Colloids Surfaces A Physicochem. Eng. Asp.* **2017**, *521*, 231.

(18) Nabavi, S. A.; Vladisavljević, G. T.; Gu, S.; Manović, V. Semipermeable Elastic Microcapsules for Gas Capture and Sensing. *Langmuir* **2016**, *32*, 9826.

(19) Xie, Y.; Wang, T. T.; Liu, X. H.; Zou, K.; Deng, W. Q. Capture and Conversion of CO_2 at Ambient Conditions by a Conjugated Microporous Polymer. *Nat. Commun.* **2013**, *4*, 1960.

(20) Nabavi, S. A.; Vladisavljević, G. T.; Zhu, Y.; Manović, V. Synthesis of Size-Tunable CO_2-Philic Imprinted Polymeric Particles (MIPs) for Low-Pressure CO_2 Capture Using Oil-in-Oil Suspension Polymerization. *Environ. Sci. Technol.* **2017**, *51*, 11476.

(21) Fayemiwo, K. A.; Vladisavljević, G. T.; Nabavi, S. A.; Benyahia, B.; Hanak, D. P.; Loponov, K. N.; Manović, V. Nitrogen-Rich Hyper-Crosslinked Polymers for Low-Pressure CO_2 Capture. *Chem. Eng. J.* **2018**, *334*, 2004.

(22) Erdem, B.; Hunsicker, R. A.; Simmons, G. W.; Sudol, E. D.; Dimonie, V. L.; El-Aasser, M. S. XPS and FTIR Surface Characterization of TiO_2 Particles Used in Polymer Encapsulation. *Langmuir* **2001**, *17*, 2664.

(23) Van Der Giesen, C.; Meinrenken, C. J.; Kleijn, R.; Sprecher, B.; Lackner, K. S.; Kramer, G. J. Generation with Humidity Swing Direct Air Capture of CO_2 versus MEA-Based Postcombustion Capture. *Environ. Sci. Technol.* **2017**, *51*, 1024.

(24) von der Assen, N.; Jung, J.; Bardow, A. Life-Cycle Assessment of Carbon Dioxide Capture and Utilization: Avoiding the Pitfalls. *Energy Environ. Sci.* **2013**, *6*, 2721.

(25) Jolliet, O.; Margni, M.; Charles, R.; Humbert, S.; Payet, J.; Rebitzer, G.; Rosenbaum, R. IMPACT 2002+: A New Life Cycle Impact Assessment Methodology. *Int. J. Life Cycle Assess.* **2003**, *8*, 324.

(26) Sing, K. S. W. Reporting Physisorption Data for Gas/Solid Systems with Special Reference to the Determination of Surface Area and Porosity (Recommendations 1984). *Pure Appl. Chem.* **1985**, *57*, 603.

(27) Weidenthaler, C. Pitfalls in the Characterization of Nanoporous and Nanosized Materials. *Nanoscale* **2011**, *3*, 792.

(28) Zhao, Y.; Shen, Y.; Bai, L.; Hao, R.; Dong, L. Synthesis and CO_2 Adsorption Properties of Molecularly Imprinted Adsorbents. *Environ. Sci. Technol.* **2012**, *46*, 1789.

(29) Sherrington, D. C. Preparation, Structure and Morphology of Polymer Supports. *Chem. Commun.* **1998**, 2275.

(30) Mane, S.; Ponrathnam, S.; Chavan, N. Effect of Chemical Crosslinking on Properties of Polymer Microbeads: A Review. *Can. Chem. Trans.* **2016**, *3*, 473.

(31) Nabavi, S. A.; Vladisavljević, G. T.; Eguagie, E. M.; Li, B.; Georgiadou, S.; Manović, V. Production of Spherical Mesoporous Molecularly Imprinted Polymer Particles Containing Tunable Amine Decorated Nanocavities with CO_2 Molecule Recognition Properties. *Chem. Eng. J.* **2016**, *306*, 214.

(32) Furukawa, H.; Yaghi, O. M. Storage of Hydrogen, Methane, and Carbon Dioxide in Highly Porous Covalent Organic Frameworks for Clean Energy Applications. *J. Am. Chem. Soc.* **2009**, *131*, 8875.

(33) Mane, S.; Gao, Z. Y.; Li, Y. X.; Liu, X. Q.; Sun, L. B. Rational Fabrication of Polyethylenimine-Linked Microbeads for Selective CO_2 Capture. *Ind. Eng. Chem. Res.* **2018**, *57*, 250.

(34) Mane, S.; Li, Y. X.; Xue, D. M.; Liu, X. Q.; Sun, L. B. Rational Design and Fabrication of Nitrogen-Enriched and Hierarchical Porous Polymers Targeted for Selective Carbon Capture. *Ind. Eng. Chem. Res.* **2018**, *57*, 12926.

(35) Kim, H.; Cho, H. J.; Narayanan, S.; Yang, S.; Furukawa, H.; Schiffres, S.; Li, X.; Zhang, Y. B.; Jiang, J.; Yaghi, O. M.; et al. Characterization of Adsorption Enthalpy of Novel Water-Stable Zeolites and Metal-Organic Frameworks. *Sci. Rep.* **2016**, *6*, 19097.

(36) Patel, H. A.; Hyun Je, S.; Park, J.; Chen, D. P.; Jung, Y.; Yavuz, C. T.; Coskun, A. Unprecedented High-Temperature CO_2 Selectivity in N_2-Phobic Nanoporous Covalent Organic Polymers. *Nat. Commun.* **2013**, *4*, 1357.

(37) Kim, Y. E.; Moon, S. J.; Yoon, Y. Il; Jeong, S. K.; Park, K. T.; Bae, S. T.; Nam, S. C. Heat of Absorption and Absorption Capacity of CO_2 in Aqueous Solutions of Amine Containing Multiple Amino Groups. *Sep. Purif. Technol.* **2014**, *122*, 112.

(38) Chen, S. P.; Sun, X.; Luo, X.; Liang, Z. CO_2 Adsorption on Premodified Li/Al Hydrotalcite Impregnated with Polyethylenimine. *Ind. Eng. Chem. Res.* **2019**, *58*, 1177.

(39) Koutsianos, A.; Kazimierska, E.; Barron, A.R.; Taddei, M.; Andreoli, E. A New Approach to Enhancing the CO_2 capture Performance of Defective UiO-66 *via* Post-Synthetic Defect Exchange. *Dalton Trans.* **2019**, *48*, 3349.

(40) Wang, X.; Zhao, Y.; Wei, L.; Zhang, C.; Jiang, J. X. Nitrogen-Rich Conjugated Microporous Polymers: Impact of Building Blocks on Porosity and Gas adsorption. *J. Mater. Chem. A.* **2015,** *3,* 21185.

(41) Dawson, R.; Cooper, A. I.; Adams, D. J. Nanoporous Organic Polymer Networks. *Prog. Polym. Sci.* **2012**, *37*, 530.

(42) Mohanty, P.; Kull, L. D.; Landskron, K. Porous Covalent Electron-Rich Organonitridic Frameworks as Highly Selective Sorbents for Methane and Carbon Dioxide. *Nat. Commun.* **2011**, *2*, 401.

(43) Saleh, M.; Lee, H. M.; Kemp, K. C.; Kim, K. S. Highly Stable CO_2/N_2 and CO_2/CH_4 Selectivity in Hyper-Cross-Linked Heterocyclic Porous Polymers. *ACS Appl. Mater. Interfaces* **2014**, *6*, 7325.

(44) Yang, B.; Liu, Y.; Li, M. Separation of CO_2-N_2 Using Zeolite NaKA with High Selectivity. *Chin. Chem. Lett.* **2016**, *27*, 933.

(45) Perera, M. S. A.; Gamage, R. P.; Rathnaweera, T. D.; Ranathunga, A. S.; Koay, A.; Choi, X. A Review of CO_2-Enhanced Oil Recovery with a Simulated Sensitivity Analysis. *Energies* **2016**, *9*, 481.

(44) Funari, C. S.; Carneiro, R. L.; Khandagale, M. M.; Cavalheiro, A. J.; Hilder, E. F. Acetone as a Greener Alternative to Acetonitrile in Liquid Chromatographic Fingerprinting. *J. Sep. Sci.* **2015**, *38*, 1458.

Graphical Abstract